Heterogenous Diffusion and Reaction Model of Kraft Delignification at the Cell Wall Level

I&EC research
Industrial & Engineering Chemistry Research

pubs.acs.org/IECR
Article

Heterogenous Diffusion and Reaction Model of Kraft Delignification at the Cell Wall Level

Linus Kron, Merima Hasani,* and Hans Theliander

Cite This: https://doi.org/10.1021/acs.iecr.4c03900

ABSTRACT: This work explores the interplay between reaction and mass transfer kinetics during kraft pulping of birch wood meal. A novel delignification model has been developed, incorporating molecular weight-based diffusivities alongside traditional reaction kinetics to describe delignification at the cell wall level. Laboratory-scale reactor experiments provided pulping data for model validation at a range of industrially relevant process conditions. The developed model successfully described the delignification behavior during both constant and transient process conditions. By fitting the model to experimental data, the calculated rate constants (for both reaction and diffusion) revealed that the rate of delignification at the cell wall level is controlled by the diffusion of dissolved lignin. The results provide a plausible explanation to the slow rate of delignification at the end of the cooking operation. Furthermore, the reaction rate may also be limited by the access to OH^- within the cell wall even during wood meal pulping.

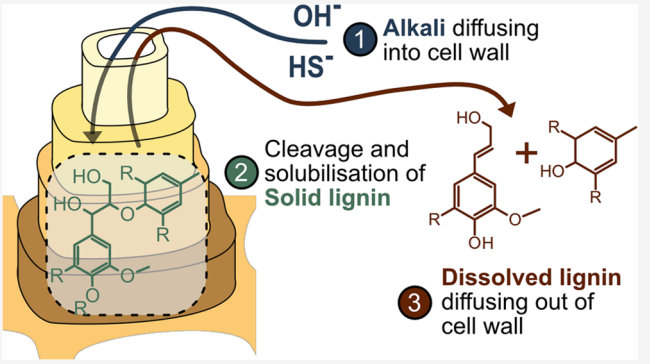

1. INTRODUCTION

Increasing the use of biobased resources is a crucial step toward reducing reliance on fossil carbon. Lignocellulosic plants, such as wood, are important raw material feedstocks due to their abundance, as well as the compositional and structural diversity of their components. These qualities enable their use in various applications, including construction, packaging, and specialty chemical production.[1] However, the complexity of wood also hinders its efficient utilization, as refining one component often compromises others, due to the difficulty of separating components while retaining their desired properties.[2] This challenge is evident in the kraft process, which accounts for over 80% of global pulp production from wood.[3] Yet, the material efficiency of a conventional kraft pulp mill is typically around 50%, making it a critical target for process improvements.

The defining step of the kraft process is delignification, where a substantial portion of lignin is removed after solubilization through the cleavage of intralignin bonds using OH^- and HS^- as active chemicals. Figure 1 provides a schematic illustration of the main stages of the delignification process. In brief, delignification involves the transport of OH^- and HS^- ions through the porous network of connected lumens, vessels, and rays inside the wood chip, followed by diffusion into the cell walls of the fibers, where they react to cleave lignin interunit linkages (mainly aryl ether bonds).[2] This cleavage reduces the molecular weight of lignin and introduces hydrophilic groups, allowing lignin fragments to dissolve and be transported out through the cell wall and via the porous network.

However, several factors can influence delignification, such as the limited availability of OH^- due to its consumption in competing reactions (e.g., peeling, hydrolysis, and deacetylation of carbohydrates);[4] the presence of components that affect lignin solubility, such as extractives or dissolved ions;[5,6] and variations in the chemical and physical structure of the fibers throughout the process, which affect diffusivities and lignin-cell wall interactions.[7,8] These parallel mechanisms make delignification a highly complex process, where a full understanding has yet to be achieved.

Nevertheless, driven by the need to improve both material and energy efficiency in pulp mills, continuous research is focused on better understanding the delignification process.[9] One tool employed in these efforts is delignification modeling, which predicts various pulp properties. Early models, such as the H-factor, were based on pseudo-first-order reactions with Arrhenius-type temperature dependence and were used to account for variations in time and temperature.[10,11] However, these models failed to capture the complex behavior of kraft

Received: October 18, 2024
Revised: December 23, 2024
Accepted: December 24, 2024

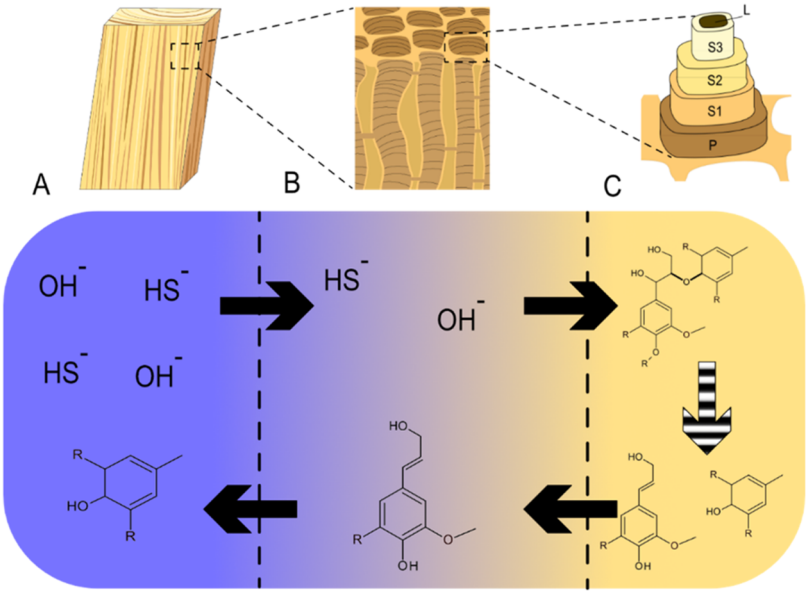

Figure 1. Schematic pathway of kraft delignification. The reactants diffuse (solid arrows) from the liquor surrounding the wood chip (A), via the network of connected lumens (B), and into the cell wall (C). There, they react with the lignin (striped arrow), cleaving interlignin bonds and solubilizing lignin fragments, which then diffuse out through the same path as the reactants.

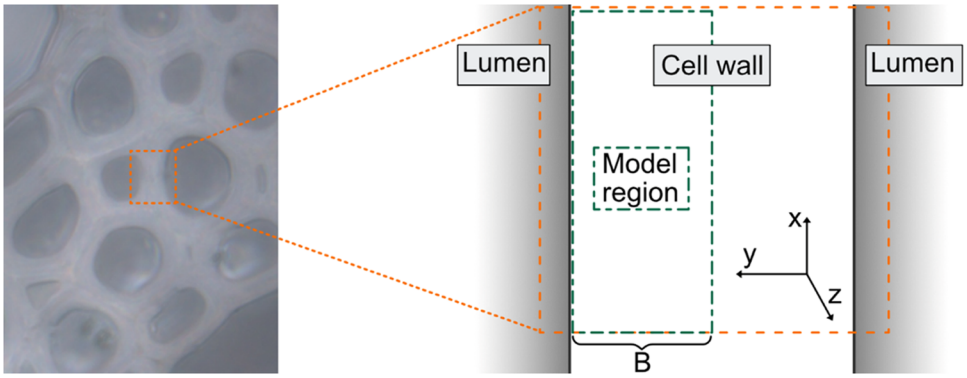

Figure 2. Illustration of the model geometry including a microscopy image of birch cell walls.

delignification. Later pseudo homogeneous models achieved improved accuracy by dividing the delignification process into different stages, each with its own kinetic expressions.[12−14] Alternatively, some models treated the components of wood as "fast" and "slow" species.[15−17]

Earlier models predominantly focused on reaction kinetics as the key determinant of kraft delignification, whereas the kinetics of mass transfer were either addressed minimally (typically alkali transport) or not at all. More recent models have broadened this scope by including desorption[18] and mass transport mechanisms[19−21] or by considering reaction expressions that account for the specific bonds and structures within lignin,[22,23] though such models remain relatively few. Factors such as chip thickness have long been known to affect delignification rates despite not influencing reaction rates directly—although they may affect alkali availability, which is itself governed by mass transport mechanisms.[24−26]

Consequently, several studies have utilized wood meal to eliminate the impact of mass transfer within the wood chip.[23,27−30] However, this approach only removes part of the mass transfer resistance: milling the wood exposes the cell walls directly to the surrounding liquor, bypassing the need for diffusion within the network of fibers (region B in Figure 1). Diffusion within the cell wall itself, however, remains significant and has been found in previous pulping studies to affect the overall rate of delignification.[31,32] Our previous work supported this, as the rate of lignin release and its molecular weight in the black liquor do not align with the trends expected from a reaction-controlled process.[33,34] Furthermore, lignin cleavage reactions appear to have little impact on kinetics after the first 10−20 min of the cook.[35]

In summary, most modeling studies of kraft delignification have thus assumed that it is a pseudo homogeneous reaction system in which the reaction is the rate-determining step. The few models incorporating mass transfer mechanisms were all performed using wood chips, and thus combine diffusion effects at different length scales (i.e., within the cell wall vs via the network of connected lumens). In addition, previous treatments of lignin diffusivity are simplified, assuming either similar behaviors to alkali,[20,36] or disregarding the heterogeneous nature of lignin and the surrounding environment.[19] Consequently, in this study, we aim to describe kraft delignification at the cell wall level of birch by hypothesizing that mass transfer of released lignin within the cell wall influences the overall delignification kinetics. A single reaction expression is combined with Fickian diffusion of the released

https://doi.org/10.1021/acs.iecr.4c03900
Ind. Eng. Chem. Res. XXXX, XXX, XXX−XXX

lignin, using a variable diffusivity that accounts for the heterogeneous nature of lignin. Kraft pulping of birch wood meal in a lab-scale flow-through reactor—representative of delignification at the cell wall level—supports model development. By employing high liquor-to-wood ratios and short residence times of the liquor flow, virtually constant concentrations can be maintained, as a series of experiments are conducted across a range of industrially relevant process conditions for model parameter estimation and validation. The goal is thus to compare the relative importance of reaction and diffusion mechanisms in a simplified system corresponding to the cell wall alone, which may offer further insights into the overall kinetics of kraft delignification.

2. MODEL DEVELOPMENT

2.1. Geometry. The concentration gradient in diffusion expressions requires a model that is resolved in both space and time. Focusing on delignification within the cell wall, the geometry was chosen to represent the wall of a single wood fiber. No distinction between cell wall and middle lamella was made in this work; instead, the wood fibers were assumed to consist solely of a homogeneous fiber wall and lumen. This assumption is justified since the majority of lignin (~80%) is located in the call wall[37]). As a result, geometrical symmetry was assumed between fibers in a bundle, with the symmetry line falling between two fiber walls (see Figure 2). Furthermore, the thickness of a single cell wall (assumed to be constant at 2.5 μm[38,39]) is relatively small compared to the radius of the fiber (~17 μm[38,40]). Therefore, the curvature of the wall was neglected, simplifying the problem to one-dimensional in space. The model region (depicted in Figure 2) is thus a slab of thickness B.

2.2. Model Equations. In its initial state, lignin is bound in a network of interunit and LCC linkages. During the delignification, parts of these linkages are cleaved, eventually resulting in lignin fragments of various sizes which will be able to diffuse out of the cell wall. In this work, the lignin remaining bonded to the network (hence unable to diffuse) is termed the solid lignin (L_S), whereas the lignin fragments which have been cleaved from the network are termed the dissolved lignin (L_D). Initially, all lignin belongs to the solid fraction, representing unreacted native lignin. The apparent rate of delignification is often reported to follow a first-order dependence on remaining lignin concentration, with rate constants derived from Arrhenius expressions.[13,15,16] However, as these studies do not distinguish between the effects of mass transfer and chemical reactions, the reported rate constants reflect the apparent rate of delignification (i.e., including the influence of mass transport), rather than the "true" rate of reaction (r_L, see eq 1). Therefore, in this work, the reaction rate constants (A_r and E_r) were determined by regression of the model to experimental data. An exception is the order of OH^- dependence (n in eq 1), which was found to have little effect on the model fit but significantly influenced its stability. As a result, it was set to first-order dependence (n = 1), based on studies of lignin model compound kinetics, which should more closely reflect the "true" reaction kinetics.[41,42] The OH^- dependence was normalized by the default concentration used in this study, i.e., OH_0 = 0.35 M.

In this work, the sulfide concentration was held constant at industrially relevant levels, as the literature on the effect of sulfidity on the delignification rate is inconclusive. It is well-known that the delignification rate increases with increasing sulfidity, albeit, beyond a certain point, further increases yield minimal additional effect. The sulfidity dependence also varies during the delignification, making it unsuitable for description using a single n-th order dependence.[13,14,28] Additionally, little research exists on how sulfidity affects lignin structure, such as molecular weight, and consequently its effect on mass transport.[43] Therefore, sulfidity dependence was excluded from the modeling in this work, but future studies will address this topic.

$$r_L = L_s\left[\frac{OH}{OH_0}\right]^n A_r e^{-E_r/RT} \quad (1)$$

As the solid lignin reacts, it is converted into the dissolved lignin fraction. This conversion represents the various reactions required to fragment the lignin into fractions small enough to start diffusing out of the cell wall. The dissolved lignin is assumed to undergo no further reactions, thus any effects of condensation or other reactions affecting the dissolved lignin during its transport through the wood tissue were neglected in this work. The dissolved lignin was removed from the cell wall solely through diffusion. Due to the heterogeneity of lignin, L_D was modeled as a distribution of fractions, $L_{D,i}$, with varying molecular weights. The distribution of $L_{D,i}$ is shown in Table 1,

Table 1. Distribution of Dissolved Lignin Fractions

dissolved lignin	M_w [Da]	relative weight, w_i	weight fraction, x_i
$L_{D,1}$	350	1	0.12
$L_{D,2}$	1.6×10^3	4.7	0.14
$L_{D,3}$	4.6×10^3	13.1	0.54
$L_{D,4}$	2.6×10^4	74.9	0.16
$L_{D,5}$	6.2×10^4	178	0.02
$L_{D,6}$	2.5×10^5	725	0.03
$L_{D,7}$	1.0×10^6	2930	0.002

based on measurements of the molecular weight distribution of dissolved birch kraft lignin presented in previous work.[34] (See Supporting Information for further discussion regarding the distribution).

The mass transport of $L_{D,i}$ was modeled to follow Fickian diffusion. However, reports on the diffusivity of lignin are scarce, and the few available values span several orders of magnitude.[44−46] Naturally, determining a single diffusion coefficient for use in delignification models is not possible. First, lignin does not exist as a defined polymer with fixed properties but as a random network of various bonds between monolignols, producing fragments with a range of moieties and molecular weights during pulping. Additionally, the diffusivity depends on interactions with the solid material, pore size, solubility, and other factors, all of which vary during the delignification process. Consequently, the diffusivity also changes throughout the process. In this work, the diffusivity was determined by fitting of the model to experimental data and adjusted for variations in three ways: molecular weight, OH^- concentration, and temperature.

To account for the molecular weight distribution (MWD) of dissolved lignin, the Stokes−Einstein theory predicts that diffusivity is inversely proportional to the hydrodynamic radius, r_H, which in turn is proportional to the molecular weight raised to a factor α, as shown in eq 2. Garver and Callaghan (1991) reported an α value of 0.39 for self-diffusion of lignin in OH_{Aq}^-, whereas a study of lignin diffusion in cellulose micropores found the relationship between diffusivity and

https://doi.org/10.1021/acs.iecr.4c03900
Ind. Eng. Chem. Res. XXXX, XXX, XXX−XXX

M_W to be closer to 1.2.[45,47] Size exclusion chromatography often uses polystyrene standards for calibration during lignin measurement, which is reported to have an α value of approximately 0.5.[48,49]

Important to note is that these values represent the apparent weight dependence of the diffusivity, which is a combination of the effect of several interactions which all affect the ability of lignin to be transported within the cell wall. For example, an increased molecular weight will negatively affect both the solubility and the steric hindrance, but possibly to different extents. During the development of this model, it was found that α = 0.5 provided the best fit to the Klason lignin experimental data. This value was therefore employed together with a M_W ratio factor w_i, as presented in Table 1 and eq 3.

$$D = \frac{k_B T}{6\pi\mu r_H}, \text{ where } \qquad r_H \propto M_w^{\alpha} \tag{2}$$

The concentration dependence of OH^- was added to account for lignin solubility and capture other mechanisms that may vary with pH, such as sorption/desorption[18] and electrostatic cell wall interactions,[7] which were not directly included in the model. Naturally, no theoretical pseudo-order m exists for the combinations of these effects, and thus this parameter was also determined through fitting of the model to experimental data.

Lastly, the temperature dependence followed an expression developed by McKibbins for diffusion in wood chips,[50] which combines both exponential and square root dependence to account for the gel-like structure of the delignified cell wall. The final expression for the diffusivity $D_{L,Di}$ is given by eq 3,

$$D_{L,Di} = D_0 \sqrt{\left(\frac{T}{T_0}\right)} e^{E_D/RT} \left[\frac{OH}{OH_0}\right]^m w_i^{-0.5} \tag{3}$$

where D_0 is analogous to the frequency factor A_r in eq 1, and T_0 is the reference temperature (413 K) employed in this work. In addition to the lignin components, the concentration of OH^- was also modeled as a separate component to account for the effects of OH^- consumption and transport within the cell wall. There is no straightforward method for modeling the consumption of OH^-, as it is influenced by numerous reactions involving both lignin and carbohydrates. However, acceptable results have been achieved using simple linear correlations between consumption and the degradation of lignin and carbohydrates.[13,15,51,52] For hardwoods, these typically result in a consumption of approximately 0.22 and 0.49 g NaOH per g lignin and "carbohydrate", respectively. The behavior of carbohydrates during delignification was outside the scope of this work and, therefore, not modeled. However, the effect of carbohydrate removal on the consumption of OH^- was included by correlating the carbohydrate degradation rate to that of solid lignin through a linear expression[13] (See Supporting Information for further details.)

The diffusivity of OH^- in wood chips has been reported to be in the in the order of 10^{-9} m^2/s at typical cooking temperatures.[2] However, the reported values differ by nearly an order of magnitude between the longitudinal and radial directions. Diffusion via the lumen and vessels can be compared to longitudinal transport, as this naturally occurs along the direction of most lumens and vessels. Diffusion within the cell wall, however, is more comparable to radial transport. Yet, it may be even slower, as radial diffusion measurements on wood chips still include transportation between lumens via pores, which are inherently less obstructed compared to transport solely through the cell wall. For example, Ghaffari et al. reported diffusivities on the order of 10^{-11} m^2/s for water in microporous cellulose membranes, where the nominal pore sizes were similar to the distances between cellulose fibril bundles within the cell wall (2−5 nm).[53] Thus, it may be reasonable to assume that diffusion of OH^- in the cell wall is of the same order of magnitude. Accordingly, in this work, the diffusivities of OH^- were set to 10^{-9} and 10^{-11} m^2/s for diffusion through the lumen/vessels and cell wall, respectively.

The developed model consisted of a system of PDEs containing nine independent variables as presented in eqs 4−6,

$$\frac{\partial L_S}{\partial t} = -r_L \tag{4}$$

$$\frac{\partial L_{D,i}}{\partial t} = D_{L_{D,i}} \frac{\partial^2 L_{D,i}}{\partial y^2} + r_L x_i, \; i = [1, 2, \cdots, 7] \tag{5}$$

$$\frac{\partial OH}{\partial t} = D_{OH} \frac{\partial^2 OH}{\partial y^2} - r_L \beta \tag{6}$$

where y is the spatial direction from the center to the surface of the cell wall, $x_{D,i}$ is the mass fraction of dissolved lignin component i, and β is the conversion factor of the rate of carbohydrate consumption relative to the rate of lignin reactions. The geometry of the model region is the slab depicted in Figure 2.

The associated boundary conditions assumed symmetry at the center of the cell wall (eq 7), and continuous non-accumulating transport at the lumen boundary (eq 8). Initial conditions are shown in eq 9.

$$\frac{\partial L_{D,i}}{\partial y} = \frac{\partial OH}{\partial y} = 0, \; y = 0 \tag{7}$$

$$\begin{cases} D_{L,w} \dfrac{\partial L_{D,w}}{\partial y} = D_{L,l} \dfrac{\partial L_{D,l}}{\partial z} \cong D_{L,l} \dfrac{L_{D,b}}{L}, \; y = B \\ D_{OH,w} \dfrac{\partial OH_w}{\partial y} = D_{OH,l} \dfrac{\partial OH_l}{\partial z} \cong D_{OH,l} \dfrac{c_0 - OH_b}{L}, \; y = B \end{cases} \tag{8}$$

$$\begin{cases} L_S = 1, \; t = 0 \\ L_{D,i} = OH = 0, \; t = 0 \end{cases} \tag{9}$$

In eqs 7−9, subscripts w, l, and b denote values inside the cell wall, lumen, and at the boundary of the two phases, respectively. The spatial direction z is along the length of the lumen, L is the length of the lumen, B is the thickness of the (single) cell wall, and c_0 is the concentration of OH^- in the cooking liquor. A linear concentration profile was assumed inside the lumen, with a negligible concentration of dissolved lignin at the end of the lumen not connected to the cell wall.

eqs 4−9 were solved numerically using the *pdepe* solver in the MATLAB environment. The model also included five parameters (A_r, E_r, D_0, E_D, and m) related to the reaction and diffusion kinetics, which were determined by fitting the model to experimental data using the nonlinear least-squares regression tool *lsqcurvefit*. For the linear regression eqs 1 and 3 were reparameterized to eqs 10 and 11, respectively, to minimize cross-correlation and reduce the difference in order

https://doi.org/10.1021/acs.iecr.4c03900
Ind. Eng. Chem. Res. XXXX, XXX, XXX−XXX

of magnitude between the parameters in order to promote the regression to converge.[51]

$$r_L = L_s\left[\frac{OH}{OH_0}\right] e^{\beta_1-\beta_2/R(\frac{1}{T}-\frac{1}{T_0})} \quad (10)$$

$$D_{L,Di} = \sqrt{\left(\frac{T}{T_0}\right)} e^{\beta_3-\beta_4/R(\frac{1}{T}-\frac{1}{T_0})}\left[\frac{OH}{OH_0}\right]^{\beta_5} w_i^{-0.5} \quad (11)$$

2.3. Experimental Section. The experimental data used for parameter regression in this work was gathered from kraft delignification of birch wood meal using a lab-scale flow-through reactor, as detailed in our previous work.[34] In summary, 4−5 g of wood was pulped at a time in the tube reactor connected to a continuous flow of cooking liquor. First, the wood was impregnated at room temperature using the same liquor as for the cook. Then, the reactor was submerged in a heated oil bath to start the delignification. The cooking liquor was preheated in the same oil bath prior to the reactor and cooled immediately after using room temperate water, thereby minimizing any further reactions of the dissolved lignin. The flow was initially set to 10 mL/min to minimize the impact of alkali-consuming reactions early in the process; after 22 min, the flow was reduced to 2.5 mL/min. Further details of the reactor setup are provided in the Supporting Material. After cooking, the pulp was washed in water until neutral and dried. For the regression of model parameters, five different process conditions were investigated at various times for a total of 25 experiments, see Table 2.

Table 2. Process Conditions

temperature [°C]	OH^- conc. [mol/kg liq]	HS^- conc. [mol/kg liq]	time [min]
140	0.35	0.15	5−180
140	0.70	0.15	5−180
150	0.35	0.15	5−180
150	0.70	0.15	5−180
160	0.35	0.15	5−180

After the cook, the pulp was analyzed for Klason lignin content following standard procedures by NREL.[54] Although the developed model involves a space-resolved distribution of different lignin fragments within the cell wall, such experimental measurements are not feasible. Instead, the measured content of Klason lignin in the pulp was compared to the total amount of lignin predicted by the model (including both the solid and dissolved fractions), summarized over the cell wall.

Additionally, for selected experiments, the dissolved lignin was precipitated from the black liquor at pH 2.5, followed by filtration, washing, and drying, as described previously.[34] The MWD of the dissolved lignin was analyzed using size exclusion chromatography, with dimethyl sulfoxide containing 10 mM LiBr as the eluent. The system used a UV detector operating at 280 nm and was calibrated with pullulan standards. For comparison with the model (which simulated the solid phase and not the black liquor), the predicted MWD of the dissolved lignin was estimated from the change in total content of each dissolved lignin fraction ($L_{D,i}$) between two time steps, corrected for the amount released by conversion of the solid lignin (L_S).

In order to validate the model, additional delignification experiments were conducted, whose results were not used in the fitting of process parameters. These validation runs were performed to assess how well the model responded to sudden changes in process conditions, as detailed in Table 3. The changes were introduced either by switching bottles for the cooking liquor feed or by moving the reactor to a differently tempered oil bath. Both types of exchanges were fully resolved within a few minutes.

Table 3. Process Conditions Used for Validation Runs

run	initial conditions	new conditions	exchange time [min]
#1	OH^-: 0.35 M T: 140 °C	OH^-: 0.35 M T: 160 °C	40
#2	OH^-: 0.70 M T: 140 °C	OH^-: 0.35 M T: 140 °C	40
#3	OH^-: 0.70 M T: 150 °C	OH^-: 0.35 M T: 140 °C	20

3. RESULTS AND DISCUSSION

3.1. Estimation of Model Parameters and Validation of the Model. Figure 3 shows the delignification over time at varying experimental conditions, alongside the corresponding results from fitting the developed diffusion and reaction-based model to the data. The model demonstrated a strong predictive capability, with an overall R^2 value of 0.997, effectively capturing the variations in both temperature and OH^- concentration.

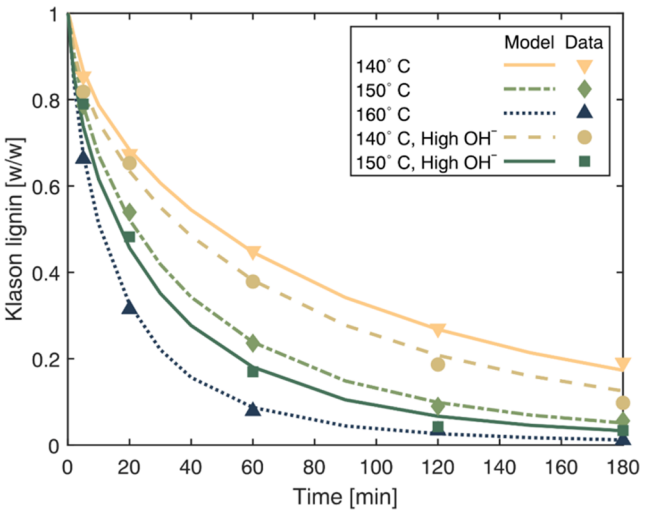

Figure 3. Fitted/predicted (lines) and experimental (points) decrease in total Klason lignin content of the pulp over time under different process conditions. The lignin content is normalized to the initial content at the start of the cook (i.e., the content in the impregnated pulp).

Figure 4 provides an example of the experimental and modeled MWD of the dissolved lignin at various residence times. The model (Figure 4A) accurately predicts the decrease in smaller fragments (<5 × 10^4 Da), which account for over 95% of the total lignin. However, it performs worse in predicting the occurrence of larger fragments (>10^5 Da), which begin to appear after 120 min. This discrepancy is somewhat expected, as the model assumes an average MWD based on the

https://doi.org/10.1021/acs.iecr.4c03900
Ind. Eng. Chem. Res. XXXX, XXX, XXX−XXX

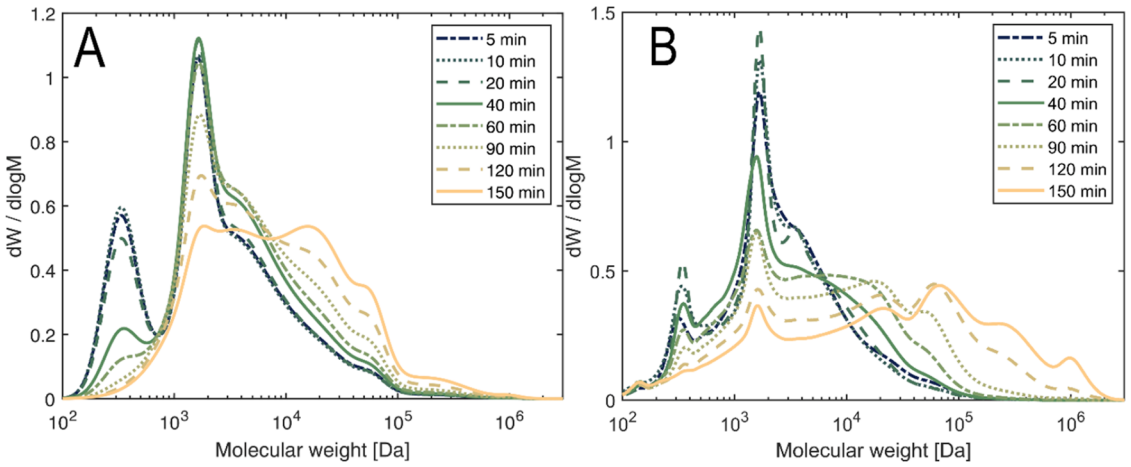

Figure 4. MWD of lignin dissolved in the black liquor after various cooking times at 150 °C and an OH^- concentration of 0.35 M, as predicted by the model (A) and obtained from the experimental data (B).

total lignin content of the wood, whereas the actual data is based on all lignin dissolved up to 150 min of cooking (corresponding to ~94% delignification). The remaining lignin likely has an even higher molecular weight than the 150 min fraction, causing the model to underestimate the weight of the released lignin, particularly toward the end of the process.

Moreover, the predicted MWD is influenced by the applied relation between hydrodynamic radius and molecular weight (α in eq 2). A higher α value results in a greater M_W dependence of the diffusivities, leading to larger differences in the MWD over time. This would cause the larger fractions to dominate more in the later stages, and the profile would resemble that of the experimental data in Figure 4B more closely. However, the α was kept at 0.5 in this work, as this value achieved the optimal fit for the delignification data (Figure 3) while simultaneously representing the MWD reasonably well. Therefore, the model is not explicitly optimized against the fit for the MWD data.

The best-fit regression estimation of the process parameters is presented in Table 4. Notably, the calculated rate of reaction

Table 4. Calculated Values for the Process Parameters Assigned through Regression

A_r [s^{-1}]	$E_r\left[\frac{kJ}{mol}\right]$	D_0 [m^2/s]	$E_D\left[\frac{kJ}{mol}\right]$	m
2.3×10^5	56.9	1.5	118.5	0.352
Calculated reaction rate and diffusivity at 150 °C, 0.35 M OH^- and $L_S = 1$				
$r_L = 2.1 \times 10^{-2}$ s^{-1}		$D_{L,Di} = 6.5–350 \times 10^{-17}$ m^2/s		

is considerably higher than previously reported values for the "apparent" rate of reaction, which includes mass transfer and other phenomena.[18,55,56] Kinetic studies using lignin model compounds—representing a closer approximation of the "true" reaction kinetics—reported rates similar to the model developed in this work.[57] However, other model studies report much lower values.[41,58] Efforts were made during fitting of the model parameters to identify any other potential local minima that would result in a lower rate of reaction than those reported in Table 4. Using a constraint on the reaction rate, another locally optimized parameter set was detected resulting in a slower reaction. Nevertheless, this set resulted in a much worse fit of the model. Further details regarding this are included in the Supporting Information.

In addition, the reaction activation energy presented in Table 4 is considerably lower than earlier reports for hardwood delignification.[14,59] However, these reported activation energies include the effects of mass transfer as part of the "apparent" reaction, whereas in this work, they are separated. In contrast, the calculated activation energy for the diffusivity is close to that of the previously reported apparent activation energy for Birch.[14] Nevertheless, the "true" activation energy of the reaction rate could likely differ considerably from the value presented in Table 4. Whereas the presented E_r is the optimal value from fitting of the model, an analysis of the confidence interval of the estimated parameters shows that E_r has a very low statistical significance in the current model. This likely stems from the reaction rate having a limited impact on the overall kinetics, and thus the temperature dependence of the diffusivity is sufficient to describe the variations of the overall delignification rate at different temperatures. Further details regarding the variance and correlation among regression parameters are included in the Supporting Material.

The existing literature on lignin diffusivity under kraft cooking conditions is limited. While previous studies examined the leaching of alkali lignin from kraft pulp, these were performed only at low to moderate temperatures (i.e., washing conditions).[44,60] In addition, the estimation of diffusivities rely on the model applied for their calculation, making direct comparisons with the values in Table 4 difficult. Nonetheless, Li et al. also reported a distribution of diffusivities attributed to the MWD of the lignin. Favis reported diffusivities similar to Li et al.'s values, and found an exponential temperature dependence of the diffusivity. Using the reported temperature dependence, extrapolation of these data to the conditions in our work yields diffusivities in the same order of magnitudes.

It is important to note that reported physical data, such as those in Table 4, are model-dependent, and should be applied with caution outside the context of their corresponding models. A simplistic sensitivity analysis of the model was conducted by independently varying the assigned parameters. Regardless of these variations, the model yielded consistent conclusions: the overall delignification kinetics of wood meal are dominated by the diffusion of dissolved lignin within the cell wall, which can be accurately described using a M_W-based diffusivity model including a relatively fast fragmentation and solubilization kinetics step. More details on the sensitivity analysis are provided in the Supporting Information.

https://doi.org/10.1021/acs.iecr.4c03900
Ind. Eng. Chem. Res. XXXX, XXX, XXX−XXX

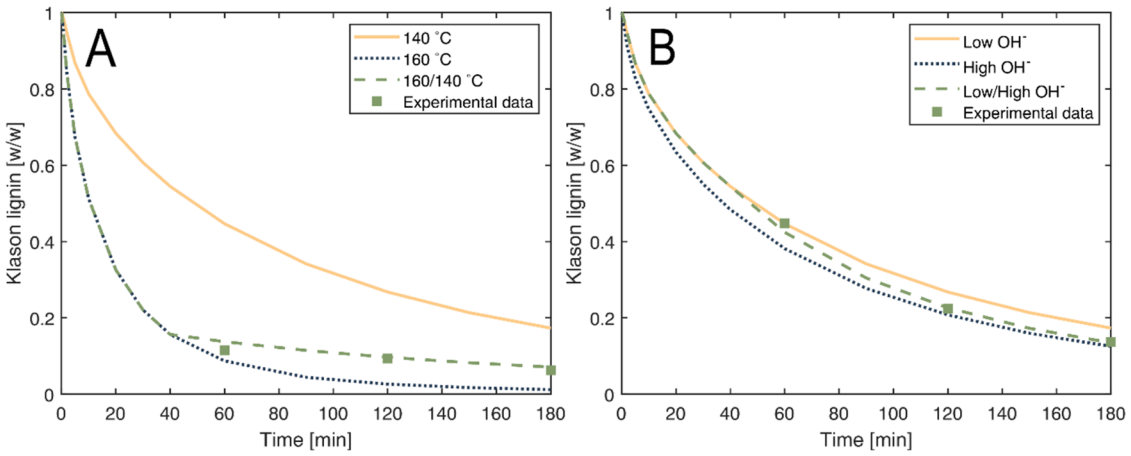

Figure 5. Residual Klason lignin content in the pulp over time. The lines represent the model predictions for both steady-state conditions and transient changes when switching from (A) low to high OH^- concentration and (B) high to low temperature. Point data correspond to experimental verification of the transient runs, which were not used in the regression of the model. Both exchanges occurred after 40 min.

The delignification model was validated using experimental data which was not used in the regression of the model parameters, while simultaneously testing the model's ability to predict transient changes in cooking conditions. The results of the validation runs are displayed in Figures 5 and 6,

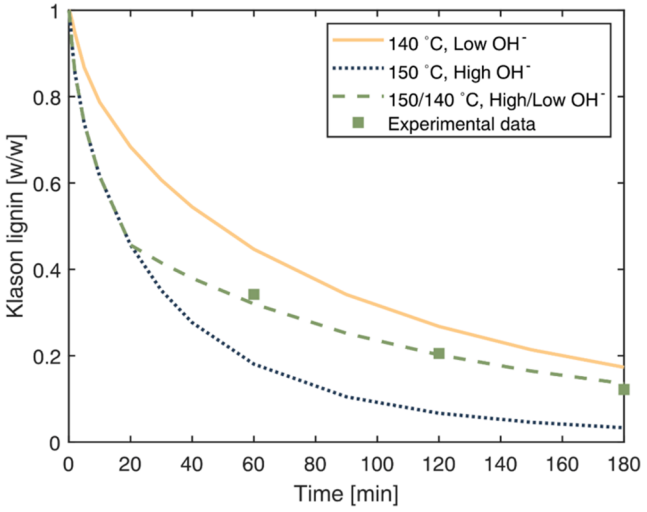

Figure 6. Residual Klason lignin content in the pulp over time. The lines show the model predictions for the steady-state conditions and for the transient change from high OH^- concentration and mid temperature to low OH^- concentration and low temperature. Point data correspond to experimental verification of the transient runs, which were not used in the regression of the model. The exchange occurred after 20 min.

demonstrating that the model performed well even under transient conditions. In Figure 5, the model slightly overestimates the response at the beginning of the exchange. This is reasonable, given that the model assumes an instantaneous exchange between the two process conditions, whereas in reality, the exchange takes a few minutes. This behavior is not seen in Figure 6, likely because the exchange occurs earlier, after 20 min, when the liquor flow in the reactor was higher compared to after 40 min, leading to a faster exchange in the experimental data (see Kron et al., 2024, for details regarding the reactor setup). Nevertheless, in both cases, the model aligns well with the later points, achieving a total R^2 value of 0.986 across all three validation predictions.

3.2. Delignification Behavior. The modeled degradation of the solid lignin is shown in Figure 7A. As expected from the high rate of reaction reported in Table 4, the degradation of solid lignin was completed after approximately 5 min of cooking, aligning with the results of Mattsson et al., who found lignin to mainly react during the first 10−20 min (using spruce wood meal). Figure 7B displays the concentration of OH^- inside the cell wall, showing that the OH^- increase closely follows the same (but inverse) rate as the degradation of solid lignin, implying that the transportation of OH^- into the cell wall occurs at a rate comparable to the rate of reaction.

To investigate whether the availability of OH^- limited the reaction rate, the model parameters for cell wall and lumen diffusivity of OH^- were varied. This led to an increased degradation rate, implying that the reaction is limited by alkali transport in the model (although both processes are relatively fast compared to the diffusion of dissolved lignin). Similar results were observed when reducing the consumption factor β or adjusting the dimensions of the model geometry, both of which improved alkali availability. Moreover, Donnan theory predicts that the actual concentration of OH^- is lower at the negatively charged fiber wall compared to the bulk.[61] The effect of this phenomenon was, however, excluded in the current model. Further details regarding the impact of variations in process parameters are discussed in the Supporting Information.

Simulated concentration profiles of four of the dissolved lignin fractions are shown in Figure 8. According to the model, even the smallest fraction of dissolved lignin (Figure 8A) diffuses out of the cell wall more slowly than the conversion rate of solid lignin, indicating that the process is diffusion-controlled from the outset. As expected from a diffusion-controlled process, a gradient of dissolved lignin is established within the cell wall, which decreases over time as the dissolved fragments diffuse out. Notably, while the smaller fragments (Figure 8A,8B) are completely removed from the cell wall by the end of the cooking process (180 min), a significant portion of the larger fragments (Figure 8C,8D) remains throughout the entire cook. The remaining large lignins may provide a plausible explanation for the slow removal rate (delignification) commonly reported during the later stages of cook-

https://doi.org/10.1021/acs.iecr.4c03900
Ind. Eng. Chem. Res. XXXX, XXX, XXX−XXX

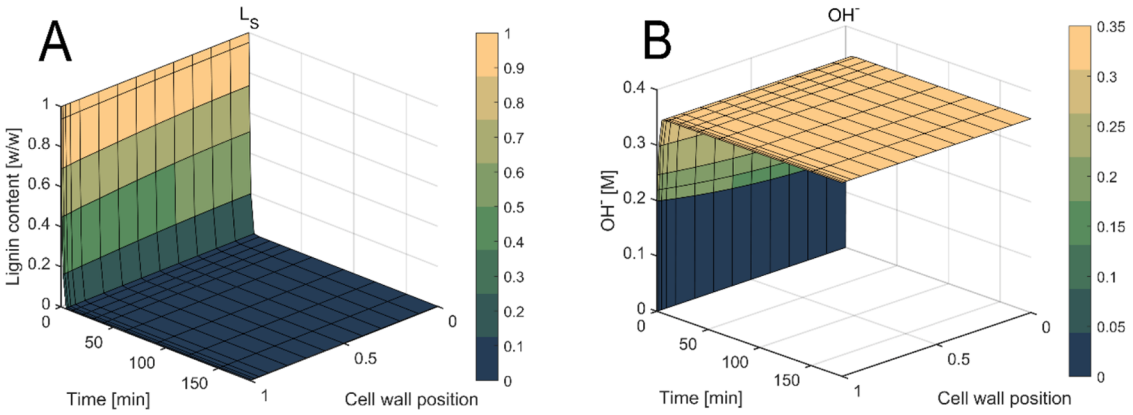

Figure 7. Predicted cell wall concentration of (A) solid lignin and (B) OH^- during 150 °C cooking at OH^- concentrations of 0.35 M.

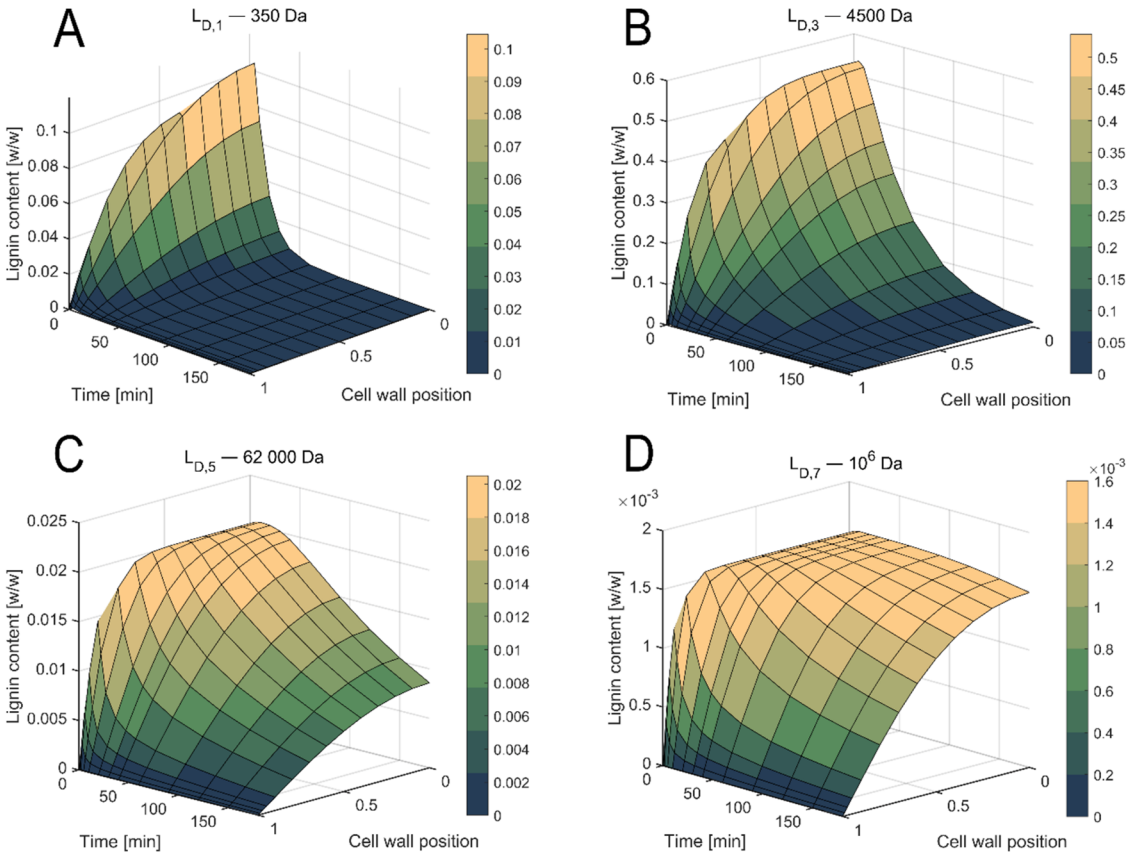

Figure 8. Predicted cell wall concentration of (A) 350 Da, (B) 4500, (C) 62 000 Da, and (D) 10^6 Da fractions of the dissolved lignin during 150 °C cooking at OH^- concentrations of 0.35 M.

ing.[24,62] The slow rate has in the literature been attributed to competing condensation reactions that counteract the fragmentation of the lignin network.[63−65] However, there has been debate regarding whether such reactions actually occur or if the observed structure of residual lignin is, in fact, native.[66,67] Regardless of whether the residual lignin is native or has undergone condensation reactions, our model suggests that the slow delignification rate at the final stage of the process is primarily due to the diffusion of these larger dissolved fragments, which have diffusivities several orders of magnitude larger than those of most other lignin fractions (as illustrated in Figure 8D).

Lastly, the concentration of all dissolved fractions in Figure 8 notably approaches zero at the boundary to the lumen/surface of the wood meal particle (i.e., at $y = 1$). Although this could be an artifact of the imposed boundary condition, it can also be physically explained by the accessibility of lignin present at the surface of the cell wall. Initially, all fragments of dissolved lignin at the surface are removed relatively easily, regardless of size (and thus diffusivity). Then, as the remaining lignin requires diffusion through the cell wall, the larger fragments begin to lag behind. This behavior is found in both the simulation and experimental results, as presented in Figure 9. Here, the average M_W of the dissolved lignin initially decreases as progressively fewer larger fragments reach the surface. Subsequently, the M_W begins to increase again, as only the larger fragments remain after the smaller ones have been depleted. The model accurately predicts the M_W during the

https://doi.org/10.1021/acs.iecr.4c03900
Ind. Eng. Chem. Res. XXXX, XXX, XXX−XXX

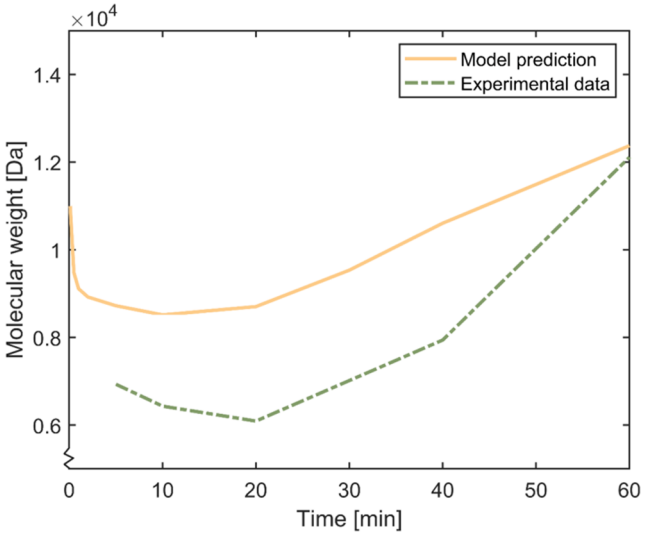

Figure 9. Comparison of the average M_W across all dissolved lignin fractions between model prediction and experimental data during the first 60 min of delignification at 150 °C (corresponding to a degree of delignification of approximately 80%).

initial stages of cooking but underestimates the M_W toward the end of the process, consistent with the results seen in Figure 4.

4. CONCLUSIONS

This work demonstrates that the rate of kraft delignification in birch wood meal can be effectively described using diffusion kinetics, specifically through a M_W-based diffusivity model that captures the heterogeneous properties of dissolved lignin. Values for the diffusivity of lignin and the intrinsic reaction rate constants were estimated by fitting the model to experimental data. The model successfully predicts the rate of delignification across the tested temperature and alkali concentration ranges, both under constant and transient process conditions, while also describing the variations in the MWD of dissolved lignin throughout the cooking process. The results suggest that the overall delignification rate is limited by the diffusion of dissolved lignin fragments, and that the rates of alkali diffusion and lignin fragmentation reactions have a relatively minor impact on the overall kinetics during birch wood meal pulping. Finally, the M_W-based diffusivity model provides a plausible explanation for the slow rate of delignification observed at the end of the process, attributing it to the remaining large fragments of dissolved lignin, which exhibit diffusivities several orders of magnitude lower than the average lignin released during the main cooking phase.

■ ASSOCIATED CONTENT

Supporting Information

The Supporting Information is available free of charge at https://pubs.acs.org/doi/10.1021/acs.iecr.4c03900.

Detailed methodology regarding calculation of dissolved lignin weight fractions and hydroxide consumption factor; sensitivity analysis and statistical analysis of regression parameters; and further details regarding experimental setup (PDF)

■ AUTHOR INFORMATION

Corresponding Author

Merima Hasani − *Department of Chemistry and Chemical Engineering, Chalmers University of Technology, SE-412 96 Gothenburg, Sweden; Wallenberg Wood Science Center, Chalmers University of Technology, SE-412 96 Gothenburg, Sweden*; Email: merima.hasani@chalmers.se

Authors

Linus Kron − *Department of Chemistry and Chemical Engineering, Chalmers University of Technology, SE-412 96 Gothenburg, Sweden*; orcid.org/0000-0003-3510-9826

Hans Theliander − *Department of Chemistry and Chemical Engineering, Chalmers University of Technology, SE-412 96 Gothenburg, Sweden; Wallenberg Wood Science Center, Chalmers University of Technology, SE-412 96 Gothenburg, Sweden*; orcid.org/0000-0002-2120-6513

Complete contact information is available at: https://pubs.acs.org/10.1021/acs.iecr.4c03900

Author Contributions

The manuscript was written through contributions of all authors. All authors have given approval to the final version of the manuscript.

Funding

This work was performed within the strategical innovation program BioInnovation—a joint initiative by Vinnova (Sweden's innovation agency), Formas (a Swedish research council for sustainable development), and the Swedish Energy Agency.

Notes

The authors declare no competing financial interest.

■ ACKNOWLEDGMENTS

Collaboration with, and the financial support of, the Resource-smart Processes Network financed by Vinnova via BioInnovation and industrial partners (Billerud, Holmen, SCA, Stora Enso, Södra Skogsägarna, and Valmet) is gratefully acknowledged.

■ ABBREVIATIONS

MWD molecular weight distribution

■ SYMBOLS

A_r	frequency factor of reaction rate constant, [s^{-1}]
B	thickness of cell wall, [m]
E_D	activation energy of lignin diffusivity, [J]
E_r	activation energy of reaction rate constant, [J]
D_0	"base diffusivity" analogous to the frequency factor A_r, [m^2/s]
D_L	diffusivity of dissolved lignin, [m^2/s]
D_{OH}	diffusivity of OH^-, [m^2/s]
L	relative length of the theoretical "Lumen" of the boundary condition, [-]
L_S	relative mass concentration of solid/unreacted lignin in the cell wall, [-]
$L_{D,i}$	relative mass concentration of dissolved/reacted lignin in the cell wall, fraction i = [1,2, ···,7], [-]
M_W	mass average molecular weight, [Da]
m	order of the OH^- dependence of the diffusivity, [-]
OH_0	reference concentration of OH^-, [M]
R	gas law constant, [J/mol K]

https://doi.org/10.1021/acs.iecr.4c03900
Ind. Eng. Chem. Res. XXXX, XXX, XXX−XXX

r_H hydrodynamic radius, [m]
r_L reaction rate of solid lignin, [s^{-1}]
T temperature, [K]
T_0 reference temperature, [K]
t time, [s]
w_i relative weight of dissolved lignin i = [1,2, ⋯, 7], [-]
$x_{D,i}$ weight fraction of dissolved lignin i = [1,2, ⋯, 7], [-]
y relative position along the thickness of the cell wall, [-]
z relative position along the length of the "lumen", [-]

SUBSCRIPTS

b Conditions at the boundary between cell wall and "lumen."
l Conditions in the "lumen."
w Conditions in the cell wall.

REFERENCES

(1) Okolie, J. A.; Nanda, S.; Dalai, A. K.; Kozinski, J. A. Chemistry and Specialty Industrial Applications of Lignocellulosic Biomass. *Waste Biomass Valorization* **2021**, *12* (5), 2145−2169.
(2) Sixta, H.; Potthast, A.; Krotschek, A. W. Chemical Pulping Processes. *Handbook of Pulp* **2006**, 109−509.
(3) FAO. *Pulp and Paper Capacities, Survey 2021−2026/Capacités de La Pâte et Du Papier, Enquête 2021−2026/Capacidades de Pulpa y Papel, Estudio 2021−2026; Rome* 2022.
(4) Brännvall, E.; Reimann, A. The Balance between Alkali Diffusion and Alkali Consuming Reactions during Impregnation of Softwood. Impregnation for Kraft Pulping Revisited. *Holzforschung* **2018**, *72* (3), 169−178.
(5) Saltberg, A.; Brelid, H.; Lundqvist, F. The Effect of Calcium on Kraft Delignification - Study of Aspen, Birch and Eucalyptus. *Nord. Pulp Pap. Res. J.* **2009**, *24* (4), 440−447.
(6) Bogren, J.; Brelid, H.; Bialik, M.; Theliander, H. Impact of Dissolved Sodium Salts on Kraft Cooking Reactions. *Holzforschung* **2009**, *63* (2), 226−231.
(7) Andersson, R.; Lidén, J.; Öhman, L.-O. The Donnan Theory Applied to Pulp Washing - Experimental Studies on the Removal of Anionic Substances from an Assumed Fiber Lumen Volume and from the Fiber Wall. *Nord. Pulp Pap. Res. J.* **2003**, *18* (4), 404−412.
(8) Wagih, A.; Hasani, M.; Hall, S. A.; Theliander, H. Micro/Nano-Structural Evolution in Spruce Wood during Soda Pulping. *Holzforschung* **2021**, *75* (8), 754−764.
(9) Mboowa, D. A Review of the Traditional Pulping Methods and the Recent Improvements in the Pulping Processes. *Biomass Convers. Biorefin.* **2024**, *14*, 1−12.
(10) Vroom, K. E. The″ H″ Factor: A Means of Expressing Cooking Times and Temperatures as a Single Variable. *PPMC* **1957**, *58*, 228−231.
(11) Hatton, J. V.Development of Yield Prediction Equations in Kraft Pulping *Tappi Tech. Ass. Pulp Pap. Indus.* 1973; Vol. *56* 7, pp 97−100.
(12) Teder, A.; Olm, L.Extended Delignification by Combination of Modified Kraft Pulping and Oxygen Bleaching *Pap. ja Puu* 1981; Vol. *63* 4a, pp 315−316.
(13) Gustafson, R. R.; Sleicher, C. A.; Mckean, W. T.; Flnlayson, B. A. Theoretical Model of the Kraft Pulping Process. *Ind. Eng. Chem. Process Des. Dev.* **1983**, *22* (1), 87−96.
(14) Lindgren, C. T.; Lindstrom, M. E. Kinetics of the Bulk and Residual Delignification in Kraft Pulping of Birch and Factors Affectingthe Amount of Residual Phase Lignin. *Nord. Pulp Pap. Res. J.* **1997**, *12* (2), 124−127.
(15) Smith, C. C. *Studies of the Mathematical Modelling, Simulation, and Control of the Operation of a Kamyr Continuous Digester for the Kraft Process*; Purdue University, 1974.
(16) Andersson, N.; Wilson, D. I.; Germgård, U. An Improved Kinetic Model Structure for Softwood Kraft Cooking. *Nord. Pulp Pap. Res. J.* **2003**, *18* (2), 200−209.
(17) Bogren, J. *Further Insights into Kraft Cooking Kinetics*; Chalmers University of Technology, 2008.
(18) Yang, L.; Liu, S. Kinetic Model for Kraft Pulping Process. *Ind. Eng. Chem. Res.* **2005**, *44* (18), 7078−7085.
(19) Simão, J. P.; Carvalho, M. G. V. S.; Baptista, C. M. S. G. Heterogeneous Studies in Pulping of Wood: Modelling Mass Transfer of Dissolved Lignin. *Chem. Eng. J.* **2011**, *170* (1), 264−269.
(20) Grénman, H.; Wärnå, J.; Mikkola, J. P.; Sifontes, V.; Fardim, P.; Murzin, D. Y.; Salmi, T. Modeling the Influence of Wood Anisotropy and Internal Diffusion on Delignification Kinetics. *Ind. Eng. Chem. Res.* **2010**, *49* (20), 9703−9711.
(21) Bijok, N.; Fiskari, J.; Gustafson, R. R.; Alopaeus, V. Modelling the Kraft Pulping Process on a Fibre Scale by Considering the Intrinsic Heterogeneous Nature of the Lignocellulosic Feedstock. *Chem. Eng. J.* **2022**, *438*, No. 135548.
(22) Kuitunen, S.; Tarvo, V.; Liitiä, T.; Rovio, S.; Vuorinen, T.; Alopaeus, V. Modeling of Alkaline Extraction Chemistry and Kinetics of Softwood Kraft Pulp. *Holzforschung* **2014**, *68* (7), 733−746.
(23) Fearon, O.; Kuitunen, S.; Ruuttunen, K.; Alopaeus, V.; Vuorinen, T. Detailed Modeling of Kraft Pulping Chemistry. Delignification. *Ind. Eng. Chem. Res.* **2020**, *59* (29), 12977−12985.
(24) Kleppe, P. Kraft Pulping. *Tappi* **1970**, *53* (1), 35−47.
(25) Agarwal, N.; Gustafson, R. A Contribution to the Modeling of Kraft Pulping. *Can. J. Chem. Eng.* **1997**, *75* (1), 8−15.
(26) Dang, V. Q.; Nguyen, K. L. A Universal Kinetic Model for Characterisation of the Effect of Chip Thickness on Kraft Pulping. *Bioresour. Technol.* **2008**, *99* (5), 1486−1490.
(27) Chiang, V. L.; Yu, J.; Eckert, R. C. Isothermal Reaction Kinetics of Kraft Delignification of Douglas-Fir. *J. Wood Chem. Technol.* **1990**, *10* (3), 293−310.
(28) Bogren, J.; Brelid, H.; Theliander, H. Reaction Kinetics of Softwood Kraft Delignification - General Considerations and Experimental Data. *Nord. Pulp Pap. Res. J.* **2007**, *22* (2), 177−183.
(29) Dang, B. T. T.; Brelid, H.; Köhnke, T.; Theliander, H. Effect of Sodium Ion Concentration Profile during Softwood Kraft Pulping on Delignification Rate, Xylan Retention and Reactions of Hexenuronic Acids. *Nord. Pulp Pap. Res. J.* **2014**, *29* (4), 604−611.
(30) Jara, R.; Lawoko, M.; van Heiningen, A. Intrinsic Dissolution Kinetics and Topochemistry of Xylan, Mannan, and Lignin during Auto-Hydrolysis of Red Maple Wood Meal. *Can. J. Chem. Eng.* **2019**, *97* (3), 649−661.
(31) Dang, B. T. T. *On the Course of Kraft Cooking The Impact of Ionic Strength*; Chalmers University of Technology, 2017.
(32) Brännvall, E.; Rönnols, J. Analysis of Entrapped and Free Liquor to Gain New Insights into Kraft Pulping. *Cellulose* **2021**, *28* (4), 2403−2418.
(33) Kron, L.; Marion De Godoy, C.; Hasani, M.; Theliander, H. Kraft Cooking of Birch Wood Chips: Differences between the Dissolved Organic Material in Pore and Bulk Liquor. *Holzforschung* **2023**, *77* (8), 598−609.
(34) Kron, L.; Hasani, M.; Theliander, H. A Comparative Study of the Cell Wall Level Delignification Behaviour of Four Nordic Hardwoods during Kraft Pulping. *Holzforschung* **2024**, *78* (8), 434−445.
(35) Mattsson, C.; Hasani, M.; Dang, B.; Mayzel, M.; Theliander, H. About Structural Changes of Lignin during Kraft Cooking and the Kinetics of Delignification. *Holzforschung* **2017**, *71* (7−8), 545−553.
(36) Bijok, N.; Fiskari, J.; Gustafson, R. R.; Alopaeus, V. Chip Scale Modelling of the Kraft Pulping Process by Considering the Heterogeneous Nature of the Lignocellulosic Feedstock. *Chem. Eng. Res. Des.* **2023**, *193*, 13−27.
(37) Fergus, B. J.; Goring, D. A. I. The Distribution of Lignin in Birch Wood as Determined by Ultraviolet Microscopy. *Holzforschung* **1970**, *24* (4), 118−124.
(38) Luostarinen, K. Relationship of Selected Cell Characteristics and Colour of Silver Birch Wood after Two Different Drying Processes. *Wood Mater. Sci. Eng.* **2006**, *1* (1), 21−28.
(39) Nilsson, J. A.; Jones, G.; Håkansson, C.; Blom, Å.; Bergh, J. Effects of Fertilization on Wood Formation in Naturally Regenerated

https://doi.org/10.1021/acs.iecr.4c03900
Ind. Eng. Chem. Res. XXXX, XXX, XXX−XXX

Juvenile Silver Birch in a Norway Spruce Stand in South Sweden. *Forests* **2021**, *12* (4), 415.
(40) Kostiainen, K.; Saranpää, P.; Lundqvist, S. O.; Kubiske, M. E.; Vapaavuori, E. Wood Properties of Populus and Betula in Long-Term Exposure to Elevated CO2 and O3. *Plant Cell Environ.* **2014**, *37* (6), 1452−1463.
(41) Gierer, J.; Ljunggren, S.Reactions of Lignin during Sulfate Pulping. Part 16. The Kinetics of the Cleavege of β-Aryl Ether Linkages in Structures Containing Carbonyl Groups *Sven. Papperstidn.* 1979; Vol. *82* 3, pp 71−81.
(42) Gierer, J.; Ljunggren, S.The Reactions of Lignin during Sulfate Pulping Part 17. Kinetic Treatment of the Formation and Competing Reactions of Quinone Methide Intermediates *Sven. Papperstidning* 1979; Vol. *17* 17, p 502.
(43) Dong, D.; Fricke, A. L. Effects of Multiple Pulping Variables on the Molecular Weight and Molecular Weight Distribution of Kraft Lignin. *J. Wood Chem. Technol.* **1995**, *15* (3), 369−393.
(44) Li, J.; Phoenix, A.; Macleod, J. M. Diffusion of Lignin Macromolecules Within the Fibre Walls of Kraft Pulp. Part I: Determination of the Diffusion Coefficient under Alkaline Conditions. *Can. J. Chem. Eng.* **1997**, *75* (1), 16−22.
(45) Ghaffari, R.; Almqvist, H.; Idström, A.; Sapouna, I.; Evenäs, L.; Lidén, G.; Lawoko, M.; Larsson, A. Effect of Alkalinity on the Diffusion of Solvent-Fractionated Lignin through Cellulose Membranes. *Cellulose* **2023**, *30* (6), 3685−3698.
(46) Zhao, X.; Wu, R.; Liu, D. Evaluation of the Mass Transfer Effects on Delignification Kinetics of Atmospheric Acetic Acid Fractionation of Sugarcane Bagasse with a Shrinking-Layer Model. *Bioresour. Technol.* **2018**, *261*, 52−61.
(47) Garver, T. M.; Callaghan, P. T. Hydrodynamics of Kraft Lignins. *Macromolecules* **1991**, *24* (2), 420−430.
(48) Li, J.; O'Hagan, T.; MacLeod, J. M. Using Ultrafiltration to Analyze the Molar Mass Distribution of Kraft Lignin at PH 13. *Can. J. Chem. Eng.* **1996**, *74* (1), 110−117.
(49) Fetters, L. J.; Hadjichristidis, N.; Lindner, J. S.; Mays, J. W. Molecular Weight Dependence of Hydrodynamic and Thermodynamic Properties for Well-Defined Linear Polymers in Solution. *J. Phys. Chem. Ref. Data* **1994**, *23* (4), 619−640.
(50) McKibbins, S. Application of Diffusion Theory to the Washing of Kraft Cooked Wood Chips. *Tappi J.* **1960**, *43* (10), 801−805.
(51) Giudici, R.; Park, S. W. Kinetic Model for Kraft Pulping of Hardwood. *Ind. Eng. Chem. Res.* **1996**, *35* (3), 856−863.
(52) Gilbert, W.; Allison, B.; Radiotis, T.; Dort, A. A Simplified Kinetic Model for Modern Cooking of Aspen Chips. *Nord. Pulp Pap. Res. J.* **2021**, *36* (3), 399−413.
(53) Ghaffari, R.; Almqvist, H.; Nilsson, R.; Lidén, G.; Larsson, A. Mass Transport of Lignin in Confined Pores. *Polymers* **2022**, *14* (10), 1993 DOI: 10.3390/polym14101993.
(54) Sluiter, A.; Hames, B.; Ruiz, R.; Scarlata, C.; Sluiter, J.; Templeton, D.; Crocker, D. *NREL/TP-510-42618 Determination of Structural Carbohydrates and Lignin in Biomass*; NREL/MRI, 2012.
(55) Chiang, V. L.; Puumala, R. J.; Takeuchi, H.; Eckert, R. E. Comparison of Softwood and Hardwood Kraft Pulping. *Tappi J.* **1988**, *71* (9), 173−176.
(56) Almeida, D.; Jameel, H.; Santos, R.; Hart, P. Hardwood Pulping Kinetics of Initial, Bulk and Residual Phases. *2014 TAPPI PEERS Conference* **2014**, *2014*, 342−352.
(57) Kondo, R.; Tsutsumi, Y.; Imamura, H. Kinetics of β-Aryl Ether Cleavage of Phenolic Syringyl Type Lignin Model Compounds in Soda and Kraft Systems. *Holzforschung* **1987**, *41* (2), 83−88.
(58) Shimizu, S.; Yokoyama, T.; Akiyama, T.; Matsumoto, Y. Reactivity of Lignin with Different Composition of Aromatic Syringyl/Guaiacyl Structures and Erythro/Threo Side Chain Structures in β-O-4 Type during Alkaline Delignification: As a Basis for the Different Degradability of Hardwood and Softwood Lignin. *J. Agric. Food Chem.* **2012**, *60* (26), 6471−6476.
(59) Santos, R. B.; Capanema, E. A.; Balakshin, M. Y.; Chang, H. M.; Jameel, H. Effect of Hardwoods Characteristics on Kraft Pulping Process: Emphasis on Lignin Structure. *BioResources* **2011**, *6* (4), 3623−3637.
(60) Favis, B. D. *The Leaching of Lignin Macromolecules from Pulp Fibres during Washing*; McGill University, 1981.
(61) Dang, B. T. T.; Brelid, H.; Köhnke, T.; Theliander, H. Impact of Ionic Strength on Delignification and Hemicellulose Removal during Kraft Cooking in a Small-Scale Flow-through Reactor. *Nord. Pulp Pap. Res. J.* **2013**, *28* (3), 358−365.
(62) Lindgren, C. T.; Lindström, M. E. The Kinetics of Residual Delignification and Factors Affecting the Amount of Residual Lignin during Kraft Pulping. *J. Pulp Pap. Sci.* **1996**, *22* (8), 290−295.
(63) Chiang, V. L.; Funaoka, M. The Dissolution and Condensation Reactions of Guaiacyl and Syringyl Units in Residual Lignin during Kraft Delignification of Sweetgum. *Holzforschung* **1990**, *44* (2), 147−156.
(64) Sjöström, E. Wood Pulping. In *Wood Chemistry: Fundamentals and Applications*, 2nd ed.; Sjöström, E. B. T.-W. C., Ed.; Academic Press: San Diego, 1993; pp 114−164.
(65) Gellerstedt, G.; Majtnerova, A.; Zhang, L. Towards a New Concept of Lignin Condensation in Kraft Pulping. Initial Results. *C. R. Biol.* **2004**, *327* (9−10), 817−826.
(66) Robert, D. R.; Bardet, M.; Gellerstedt, G.; Lindfors, E. L. Structural Changes In Lignin During Kraft Cooking Part 3.* on the Structure of Dissolved Lignins. *J. Wood Chem. Technol.* **1984**, *4* (3), 239−263.
(67) Blixt, J.; Gustavsson, C. A. S. Temperature Dependence of Residual Phase Delignification during Kraft Pulping of Softwood. *Nord. Pulp Pap. Res. J.* **2000**, *15* (1), 12−17.

https://doi.org/10.1021/acs.iecr.4c03900
Ind. Eng. Chem. Res. XXXX, XXX, XXX−XXX